

Effects of Fluid Flow Characteristics and Heat Transfer of Integrated Impingement Cooling Structure for Micro Gas Turbine


 Open
Access

Hamidon Salleh¹, Amir Khalid^{2,*}, Syabillah Sulaiman², Bukhari Manshoor¹, Izzuddin Zaman¹, Shahrin Hisham Amirnordin¹, Amirul Asyraf¹, Wahid Razzaly³

¹ Centre for Energy and Industrial Environment Studies (CEIES), Fakulti Kejuruteraan Mekanikal, Faculty of Mechanical and Manufacturing Engineering, Universiti Tun Hussein Onn Malaysia, Parit Raja, Batu Pahat, 86400 Johor, Malaysia

² Automotive and Combustion Synergies Technology Group, Faculty of Engineering Technology, Universiti Tun Hussein Onn Malaysia, 86400 Pagoh, Johor, Malaysia

³ Universiti Tun Hussein Onn Malaysia, Parit Raja, Batu Pahat, 86400 Johor, Malaysia

ARTICLE INFO

Article history:

Received 23 July 2020

Received in revised form 21 September 2020

Accepted 24 September 2020

Available online 30 September 2020

ABSTRACT

Gas turbine is one of the important sources of energy which combust a combination of fuel and compress air to produce a mechanical work that will be converted into electrical energy. Efficiency of gas turbine can be increased by raising the Turbine Inlet Temperature (TIT). The problem is current trend of TIT already exceed the allowable melting point temperature of metal blade material. The current turbine blade can withstand its high temperature by adding jet impingement cooling structure into turbine blade. The purpose of this research is to investigate the effect of combination two different stand-off distance ratio, Y/D towards the heat transfer coefficient of the target plate by using Ansys FLUENT Computational Fluid Dynamics (CFD). Combination of stand-off distance ratio, Y/D = 1.5&3.0 gave 2nd highest heat transfer coefficient on the target plate next to the original stand-off distance ratio, Y/D = 1.5 with only a slightly different in value. By combining two different stand-off distance ratio, Y/D in a set of arrays, it can affect the heat transfer coefficient on the target plate. It seems that the combination of stand-off distance may improve the performance of heat transfer coefficient of turbine blade that have relatively lower heat transfer coefficient and may be detrimental to the performance of heat transfer coefficient that have a relatively high heat transfer coefficient

Keywords:

Heat transfer coefficient; gas turbine blade; Computational Fluid Dynamics (CFD); impingement cooling

Copyright © 2020 PENERBIT AKADEMIA BARU - All rights reserved

* Corresponding author.

E-mail address: amirk@uthm.edu.my (Amir Khalid)

1. Introduction

Gas Turbines usually are used to generate power and for aircraft propulsion, and with the need for increase of power require performance of the turbine to be improved. Simple gas turbines consist of few components to operate that is compressor, combustion chamber, and turbine [1-6].

Performance of the gas turbine depends on the increasing of thermal efficiency and power output. Gas turbines and aircraft propulsion follow Brayton Cycle showing that to increase the power output, Turbine Inlet Temperature (TIT) need to be increased [7-12]. To supply the demand of power, industries have been developing very efficient gas turbine used in power plant and propulsion system with high Turbine Inlet Temperature (TIT) of 1970K or more, Funazaki [1] which exceed the allowable temperature that are over the melting point of the blade itself. Thus, cooling technology is needed so that it can ensure the lifetime of the turbine blade and safety of operation.

Latest cooling technology for the turbine blade is the thermal barrier coating and advanced integrated impingement cooling. Thermal barrier coating is made from a low thermal conductivity ceramic and act as an insulation to protect the outer layer of turbine blade by reducing the heat transfer, Padture [7]. Integrated impingement cooling is the combination of the pin-fin cooling with the film cooling so that the structure will be cooled from external and internal. This integrated cooling structure can be employed as a cooling system for ultra-high Turbine Inlet Temperature (TIT) soon. Extensive studies have been conducted by a lot of researcher to collect various data on the effect of pin-fin (shape, size, distance) and the arrangement of impingement jet so that they can improve the efficiency of Heat Transfer Coefficient (HTC) of the integrated cooling system [13-18].

In most of the cases study, distance between impingement jet and target plate was called a stand-off distance with ratio of pin height to the diameter of the impingement hole, H/d . Funazaki [8] conduct a study on heat transfer characteristic inside a cooling configuration for turbine nozzle with stand-off distance as a variable. From this study, Funazaki [8] has found that jet impingement induced high heat transfer on a target plate and since it has small distance from impingement and target plate, it produces a ring like regions of the high heat transfer on the target plate. The low heat transfer region emerged in the middle because of the jets were at the early stage of their transition to turbulence. Besides that, a stripe-shape of high heat transfer region emerged by the interaction between of two neighbouring which collide and impinge on one another. This study has been done experimentally and numerically to check the validation of the data [19-21].

Stand-off distance also can be compared to pin height because they will have the same value since it has the same distance from impingement hole to the target plate [22,23]. Cho [9] conducted a study to simulate the impingement cooling and investigate the local heat transfer on inner surface with the variation of gap distance, Reynold number and hole arrangement. Gap distance or stand-off distance is one of the factors that can affect the heat transfer coefficient of the target plate. Result from the study, Cho stated that overall heat transfer rate increases as the stand-off distance, H/d decreases. In addition, jet impingement heat transfer by Han [10] with important parameters relevant to gas turbine systems was discussed. In this paper, nozzle to plate spacing or stand-off distance is label L/D . Based on the graph of Nusselt number against nozzle to plate spacing, it can be concluded that this paper support statement from Cho that heat transfer rate increases as stand-off distance decreases.

Garimella [11] also conducted an experiment to determine the effect of nozzle-geometry in jet impingement heat transfer. Aspect ratio of L/D became the variable of testing of this experiment on effect of nozzle-geometry. From the result, heat transfer coefficient drops sharply from L/D value of 1 till 4 and increase slightly up to L/D value 8 till 12. It seems that despite the immense importance of stand-of distance in improving the heat transfer rate, almost all numerical and experimental studies on multiple jet impingement heat transfer have been focused on constant stand-of distance

ratio. The foregoing literature review found no reported studies of multiple jet impingement with combined two different stand-off distance ratio. The significance of this study is by combining two different stand-off distance ratios, the flow turbulent intensity will increase and in turn will increase the heat transfer at the target surface. The effects of key parameters such as stand-off distance (Y/D) and Reynolds Number (Re) are discussed in detail in terms of heat transfer coefficient distribution on target plate and heat transfer coefficient value on line 1, line 2 and line 3 on target plate.

2. Methodology

2.1 Reynolds Number (Re)

Reynolds number is a dimensionless quantity that help to predict the fluid flow.

$$Re = \rho U D / \mu$$

where,

ρ = Density of air (kg/m^3)

U = Velocity of air flow (m/s)

D = Impingement hole diameter (m)

μ = Dynamic viscosity of air (kg/ms)

2.2 Modelling

The based model stand-off distance with ratio Y/D 1.5 was designed with height of 30mm. The impingement hole and film hole have a diameter, D of 20mm. Diameter of pin is 12.5mm while the distance between from one jet to another jet is $5D$ and the distance from jet to pin is $2.5D$. There were 2 pin sandwiched position in between the impingement plate and the target plate. Combination of multiple stand-off distance in test model as in Figure 1 for increasing in height starting from the ratio Y/D 1.5. The model with decreasing Y/D and schematic of Model 1 with line reference are shown in Figure 2 and Figure 3, respectively.

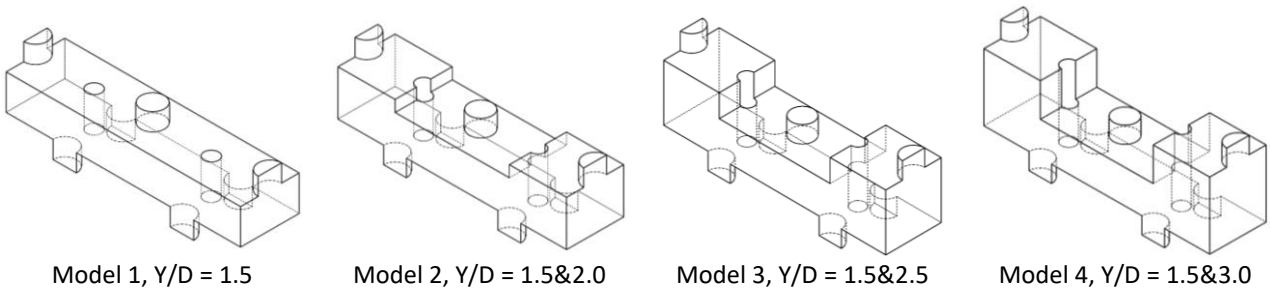


Fig. 1. Model with increasing Y/D

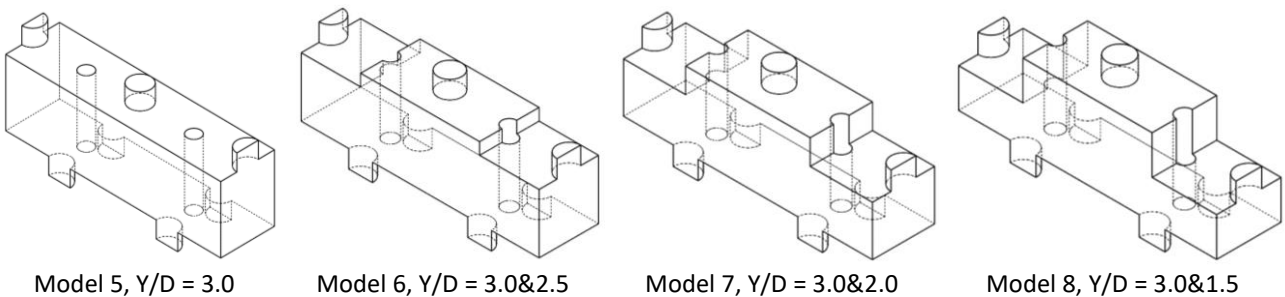


Fig. 2. Model with decreasing Y/D

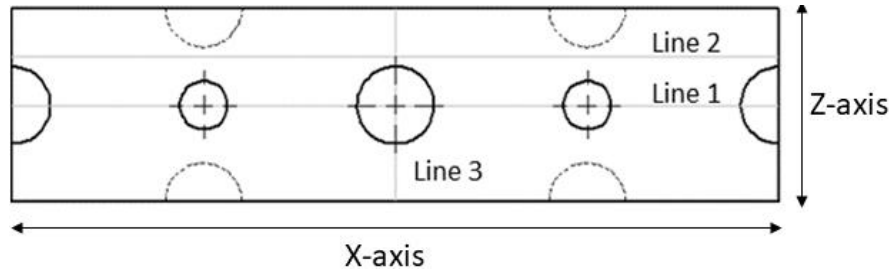


Fig. 3. Schematic of Model 1 with line reference

2.3 Meshing

Meshing used in this study was validated using the test model in numerical study by Funazaki [1] for the STAG2 model. Grid independence test was conducted to get the correct mesh size while using the multizone. The grid independence test was conducted by reducing the size of element step by step. Inlet velocity for the validation used BR=0.6 while for case study model used flow at Reynolds number 4500, 6000, 8000, 10000 to run the simulation. Presented in Figure 4, element size at 0.85 mm was chosen as it has the optimum result.

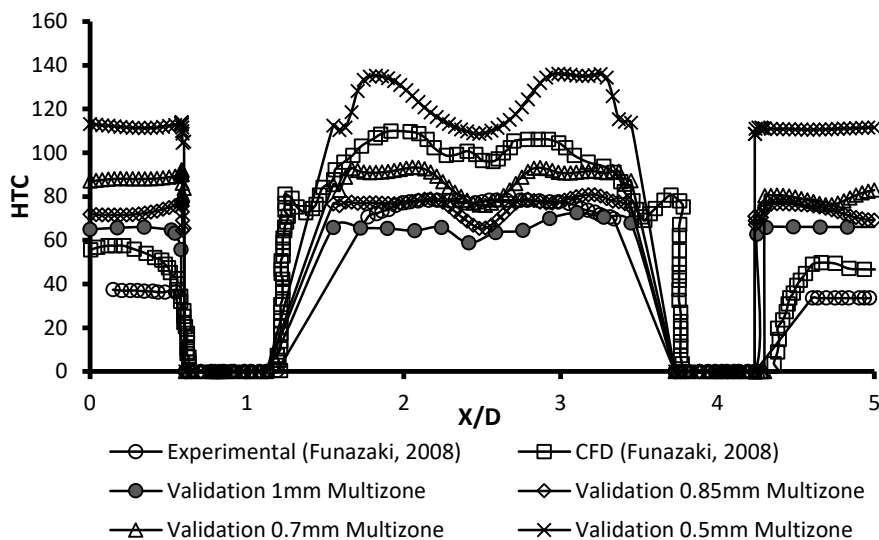


Fig. 4. Valiation of STAG2 by Funazaki [1]

2.4 Governing Equations

The flow was assumed 3-dimensional, steady state and fully developed with negligible gravitational effect. The Reynolds-Averaged Navier-Stokes equations (RANS) as following were solved

Continuity equation

$$\frac{\partial u}{\partial x} + \frac{\partial v}{\partial y} + \frac{\partial w}{\partial z} = 0 \quad (1)$$

x-momentum equation

$$\frac{\partial(\rho u)}{\partial t} + \nabla \cdot (\rho u V) = -\frac{\partial p}{\partial x} + \frac{\partial \tau_{xx}}{\partial x} + \frac{\partial \tau_{yx}}{\partial y} + \frac{\partial \tau_{zx}}{\partial z} + \rho f_x \quad (2)$$

y-momentum equation

$$\frac{\partial(\rho v)}{\partial t} + \nabla \cdot (\rho v V) = -\frac{\partial p}{\partial y} + \frac{\partial \tau_{xy}}{\partial x} + \frac{\partial \tau_{yy}}{\partial y} + \frac{\partial \tau_{zy}}{\partial z} + \rho f_y \quad (3)$$

y-momentum equation

$$\frac{\partial(\rho w)}{\partial t} + \nabla \cdot (\rho w V) = -\frac{\partial p}{\partial z} + \frac{\partial \tau_{xz}}{\partial x} + \frac{\partial \tau_{yz}}{\partial y} + \frac{\partial \tau_{zz}}{\partial z} + \rho f_z \quad (4)$$

The applicability of shear stress transport k- ω (SST k- ω) was verified during the validation process. In present work, all the setting used during the meshing and setup was the same as during the validation process since this study does not have an experimental setup. Thus, the validation only can be done by re-calculating the model from other study that is almost similar to present study case to prove that the setting and boundary condition used is suitable for it.

2.5 Boundary Conditions

Table 1 shows the boundary operating condition used for this simulation. At the solid wall, the velocity is zero due to non-slip condition. The inlet velocity, U was calculated at Re = 4500, 6000, 8000, and 10000. This corresponded to the turbulent intensity, I of 5.0%. At the outlet boundary, the pressure was set at the atmospheric pressure (0 gage pressure). The working fluid was air at 45°C with $\rho = 1.109 \text{ kg/m}^3$ and $\mu = 1.941 \times 10^{-5} \text{ kg/ms}$.

Table 1
Boundary condition

Inlet	Type	: Velocity-inlet
	Temperature (°C)	: 45
	Velocity (m/s)	: 3.514, 4.68, 6.25, 7.8
Outlet	Type	: Pressure-Outlet
	Pressure (Pa)	: 0-gauge pressure
Pin/Target Plate	Type	: Wall
	Temperature (°C)	: 25
Turbulence Model	Type	: k- ϵ (SST)
Wall	Type	: Smooth wall
	Shear condition	: No-slip

3. Result and Discussion

3.1 Analysis of Heat Transfer Coefficient at Target Plate

Analysis at the target plate with different multiple stand-off distance was conducted at condition with flow that have 4500, 6000, 8000, and 10000 Reynolds number. The analysis would involve the distribution of heat transfer coefficient, Line 1, Line 2, Line 3 and the average of heat transfer coefficient. Line 1 is the centre line across horizontal of the target plate, Line 2 is a line also across the horizontal of the target plate but with a little bit of deviation away from the centre, while Line 3 is the centre line across the target plate vertically.

Figure 5 to Figure 8 shows the distribution of heat transfer coefficient on target plate, it can be observed that there was barely any change in the middle jet section except at the distribution of decreasing stand-off distance where there is actually increasing contour representing that there were increase in heat transfer coefficient. For the jet that impinging the plate underneath that was

increasing its stand-off distance, the contour shows that the plate start to lose heat transfer coefficient while for the jet that was decreasing its stand-off distance, the contour shows the plate underneath the jet start to gain heat transfer coefficient. Figure 9 to Figure 20 show the value of local heat transfer coefficient on target plate. Heat transfer coefficient at line 1 on the target plate for every model and it seems the heat transfer rate across the middle line of horizontal shows that every model has the approximately the same heat transfer coefficient. Model 1 and 2 shows a close value of heat transfer coefficient at line 2, also the same case of model 3 which show close value with model 4. Nevertheless, the line 2 plotted graph shows that there were in fact change of heat transfer coefficient by the increasing in stand-off distance. Based on the graph, it can be said that roughly the heat transfer coefficient is decreasing for the range that is near the jet with higher stand-off distance. Heat transfer coefficient distribution at line 2 on the target plate for test model with combination of ratio Y/D decreasing in height it can be observed that the heat transfer coefficient drop slightly from model 5 to model 6 then increase from model 6 onwards till model 8. Model 5 and 6 shows a close value of heat transfer coefficient at line 2, also the same case of model 7 which show close value with model 8. Heat transfer coefficient at line 3 shows the same heat transfer coefficient at the vertical center line proving that the line is not affected by the change in height for the neighboring jet even on higher cases of Reynolds number. It can be summarized that the behavior of flow is approximately the same.

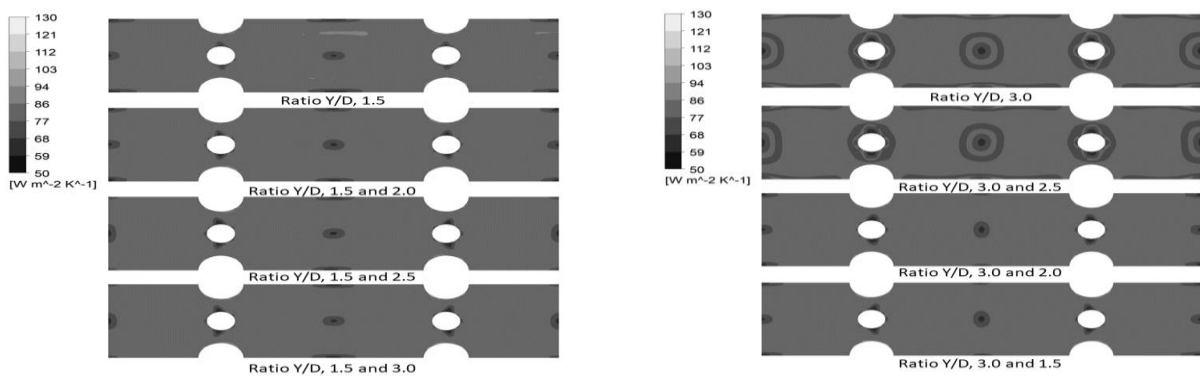


Fig. 5. Contour of heat transfer coefficient distribution with $Re=4500$ on target plate, $W/m^2 K$

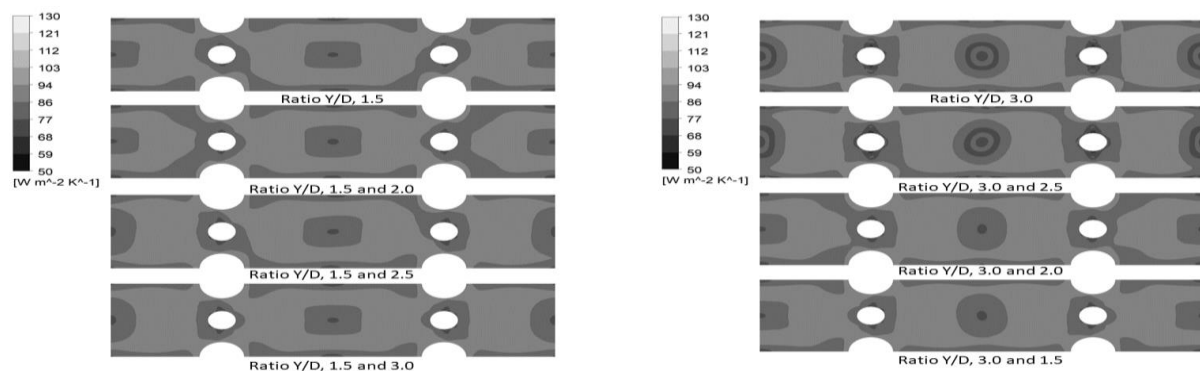


Fig. 6. Contour of heat transfer coefficient distribution with $Re=6000$ on target plate, $W/m^2 K$

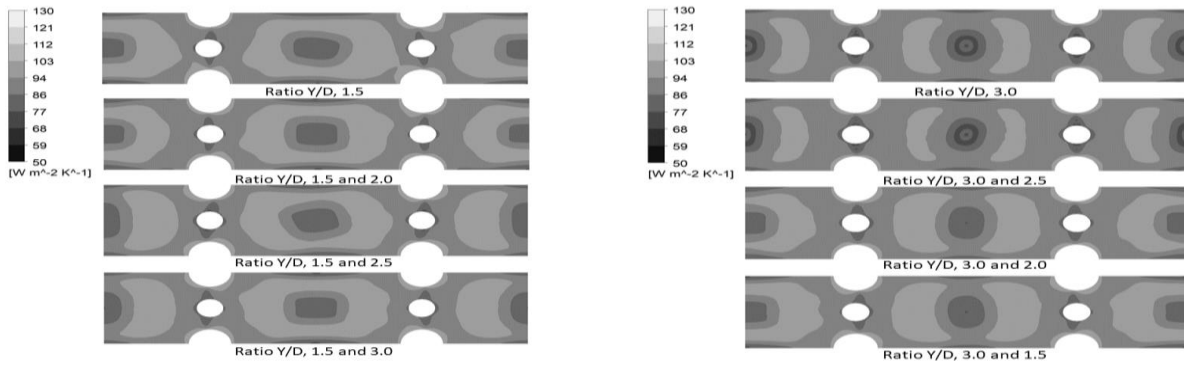


Fig. 7. Contour of heat transfer coefficient distribution with $Re=8000$ on target plate, $W/m^2 K$

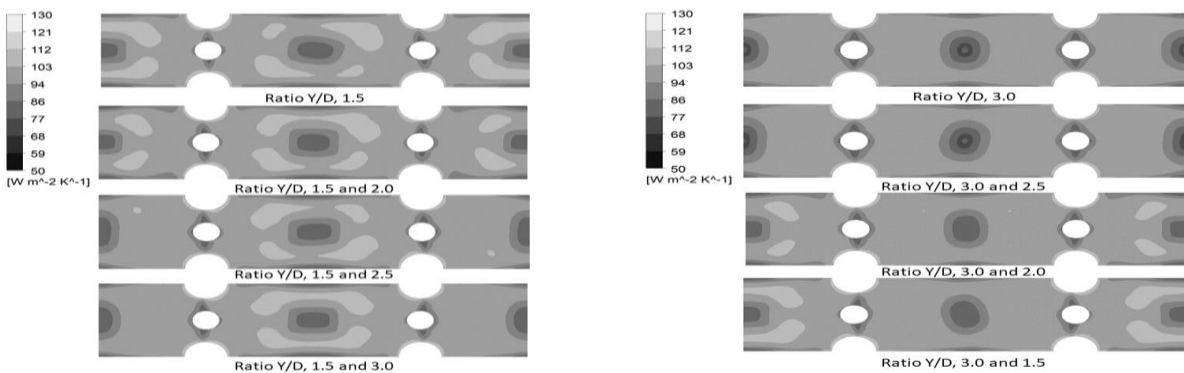


Fig. 8. Contour of heat transfer coefficient distribution with $Re=10000$ on target plate, $W/m^2 K$

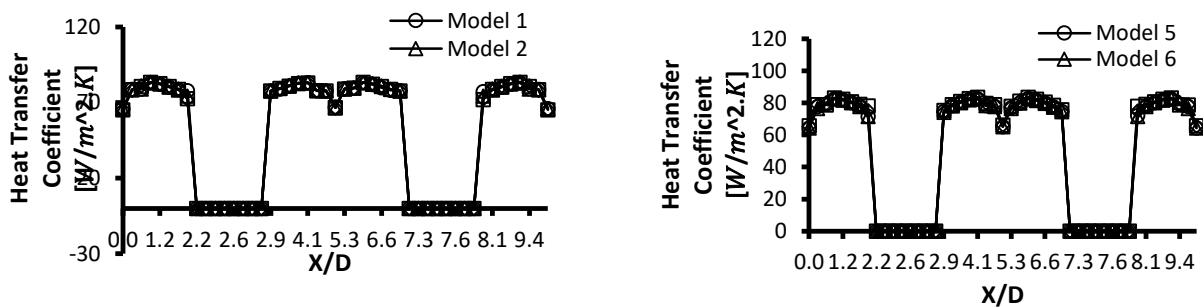


Fig. 9. Graph of Line 1 at Reynolds number 4500

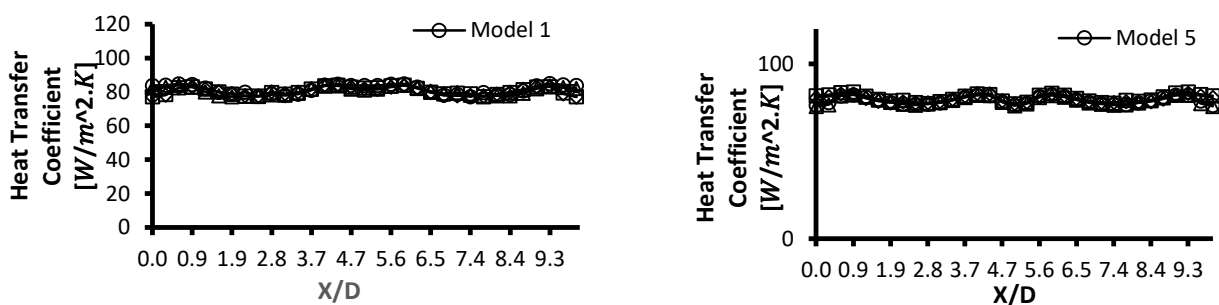


Fig. 10. Graph of Line 2 at Reynolds number 4500

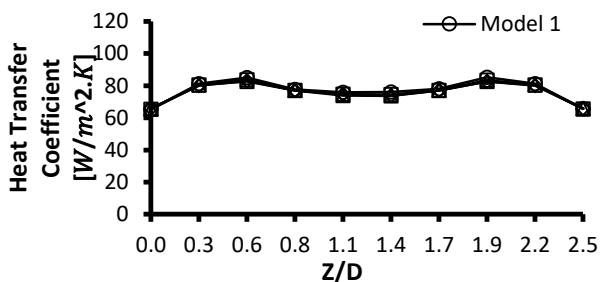


Fig. 11. Graph of Line 3 at Reynolds number 4500

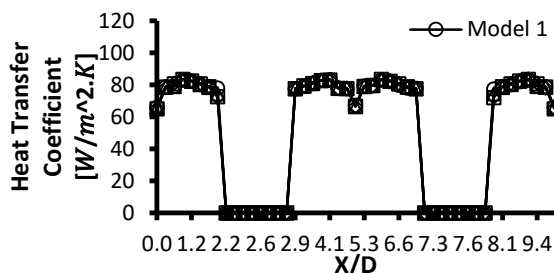
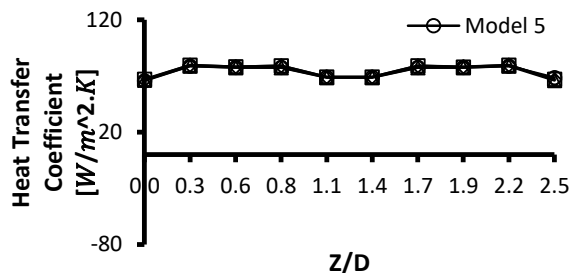


Fig. 12. Graph of Line 1 at Reynolds number 6000

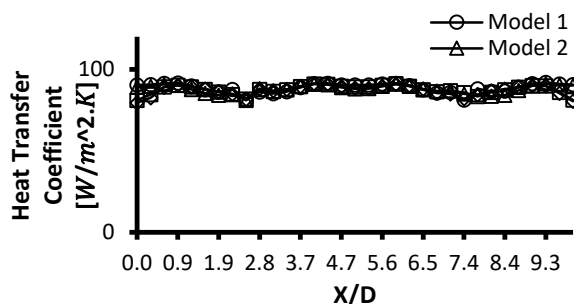
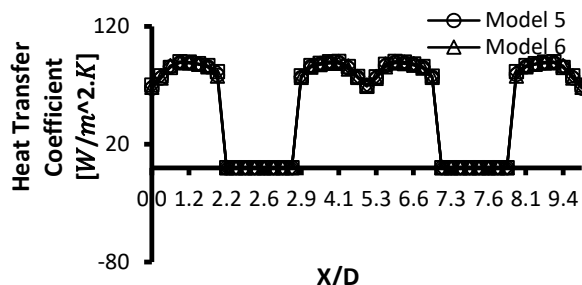


Fig. 13. Graph of Line 2 at Reynolds number 6000

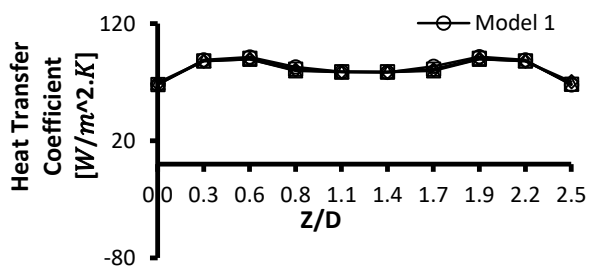
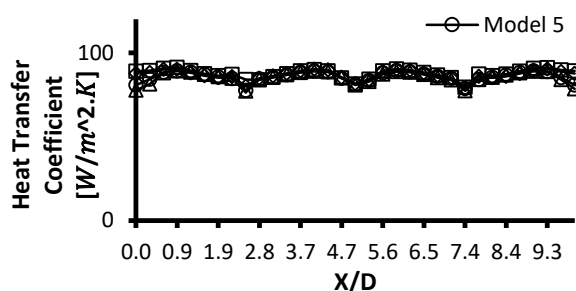


Fig. 14 Graph of Line 3 at Reynolds number 6000

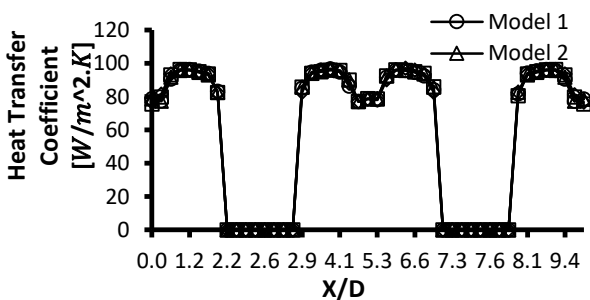
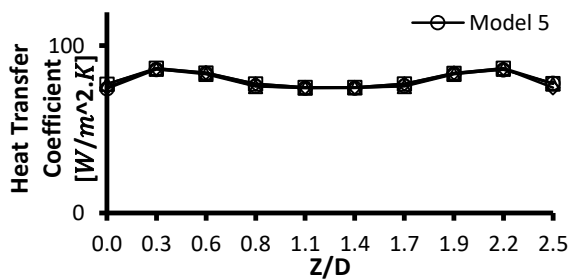
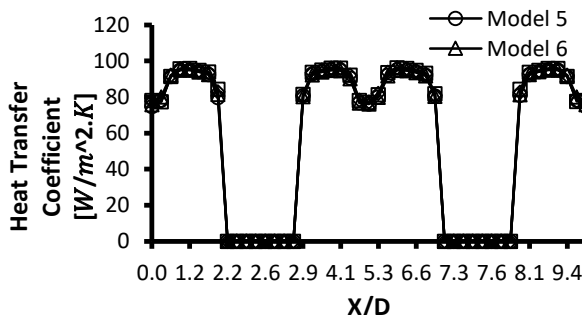


Fig. 15. Graph of Line 1 at Reynolds number 8000



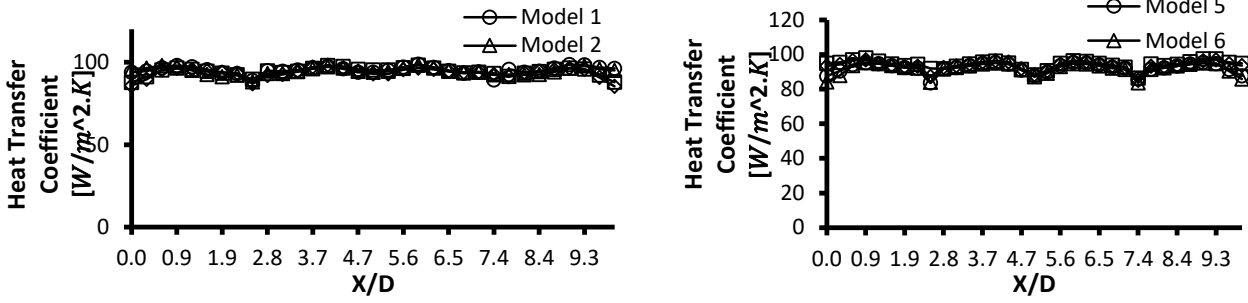


Fig. 16. Graph of Line 2 at Reynolds number 8000

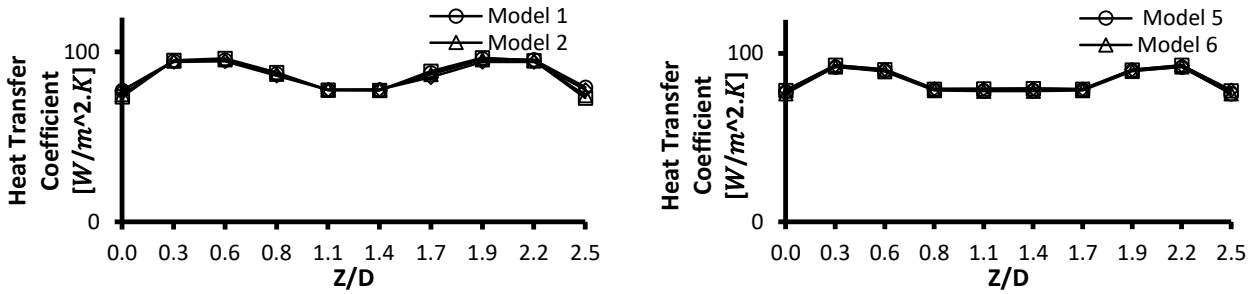


Fig. 17. Graph of Line 3 at Reynolds number 8000

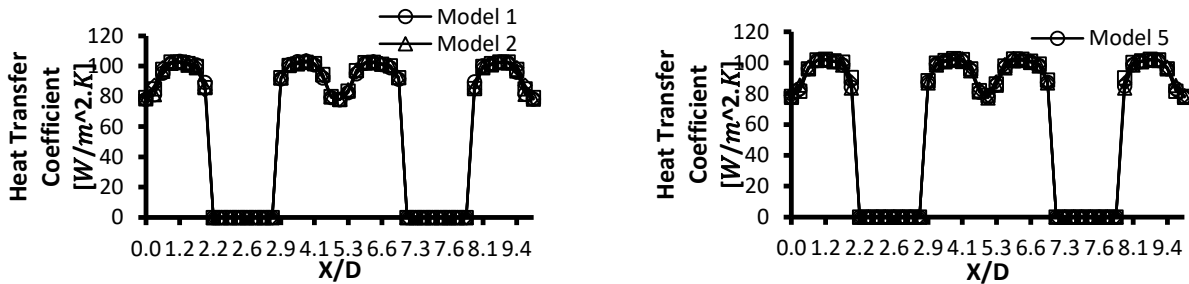


Fig. 18. Graph of Line 1 at Reynolds number 10000

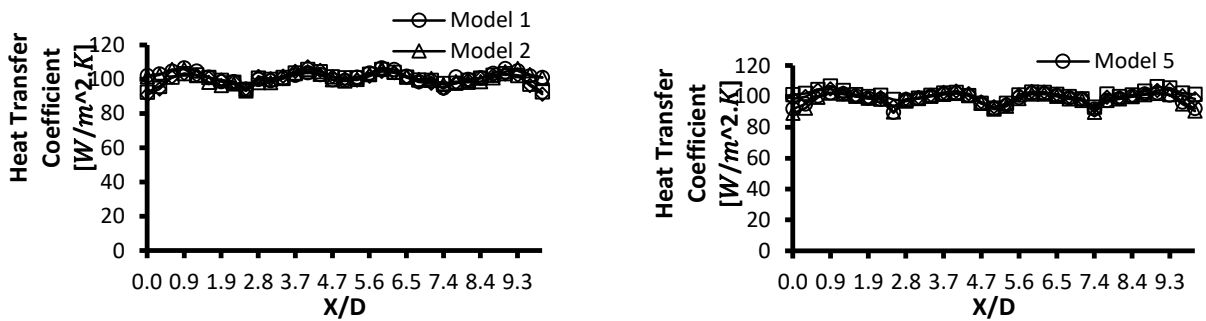


Fig. 19. Graph of Line 2 at Reynolds number 10000

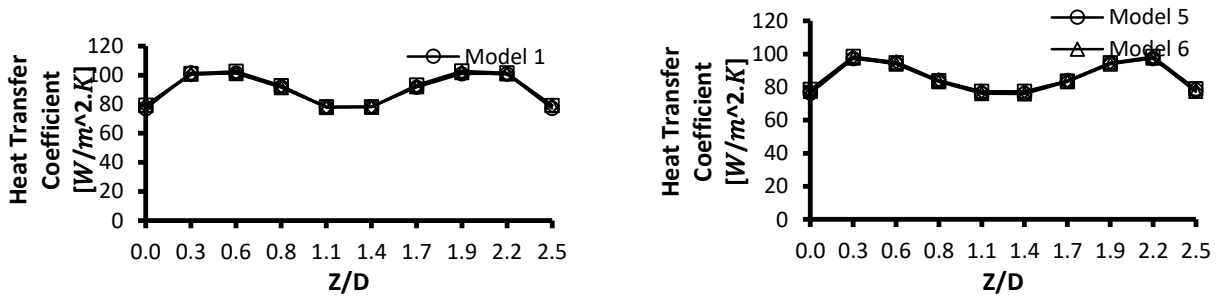


Fig. 20. Graph of Line 3 at Reynolds number 10000

Looking at the which shows the average heat transfer coefficient distribution for model with increasing stand-off distance in flow for Reynolds number = 6000, the combination of stand-off distance and increase in stand-off distance cause the average heat transfer coefficient distribution to drop from Model 1 that have ratio $Y/D = 1.5$ for every jet to Model 2 and start to increase a slightly for Model 3 and 4 but still below the average heat transfer coefficient of the original model that is have the same ratio $Y/D = 1.5$ for every jet.

Figure 21 presents the combination of different ratio Y/D with decrease in stand-off distance cause a slight unnoticeable drop in average heat transfer coefficient from Model 5 that have the original ratio $Y/D = 3.0$ for every jet to Model 6 but increase above the average heat transfer coefficient for Model 7 and Model 8 comparing with Model 5.

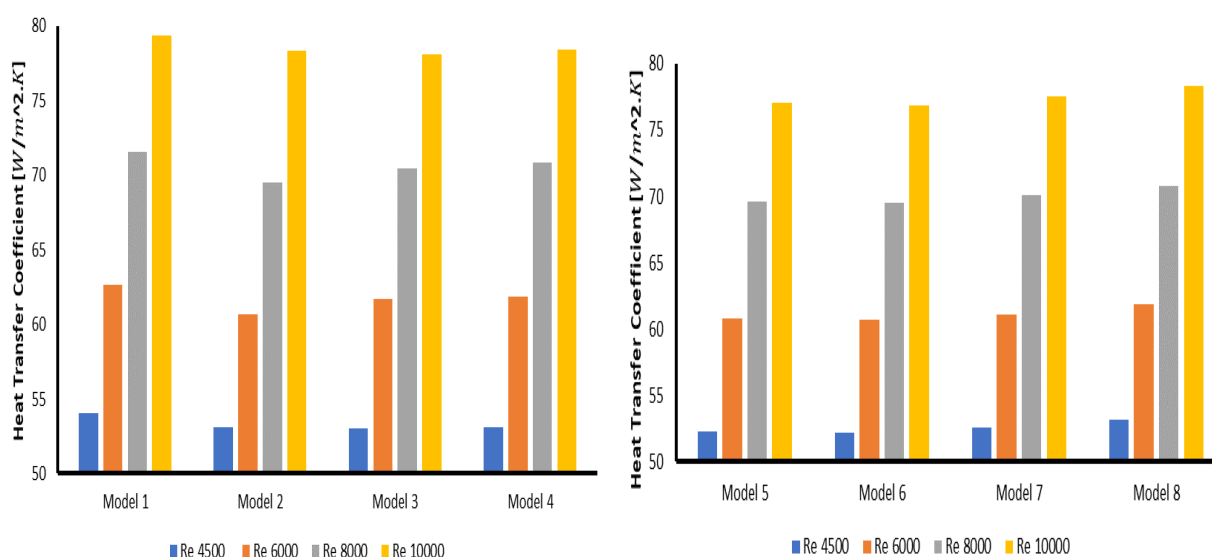


Fig. 21. Average heat transfer coefficient (HTC) at target plate

4. Conclusion

Numerical analysis of the model with combination of two stand-off distance Y/D shows that the average heat transfer coefficient distribution for increasing in height was reduced slightly from Model 1 to Model 4 while for stand-off distance Y/D that decreasing in height shows increase in average heat transfer coefficient distribution on the target plate from Model 5 to Model 6. Even though for combination of Y/D in decreasing height shows an improvement in heat transfer coefficient distribution when compared to combination of Y/D with increasing in height, but this is because of the average heat transfer coefficient for Model 1 with $Y/D = 1.5$ is a lot higher than Model 5 with $Y/D = 3.0$ around $71.5 \text{ W/m}^2.\text{K}$ to $69.6 \text{ W/m}^2.\text{K}$. In conclusion, the combination of stand-off distance may improve the performance of heat transfer coefficient of turbine blade that have relatively lower heat transfer coefficient and may be detrimental to the performance of heat transfer coefficient that have a relatively high heat transfer coefficient.

Acknowledgement

The authors would like to thank the Ministry of Education Malaysia for supporting this research under Fundamental Research Grant Scheme Vot No. FRGS/1/2019/TK10/UTHM/02/7 and partially sponsored by Universiti Tun Hussein Onn Malaysia.

References

- [1] Funazaki, Ken-ichi, and Hamidon Bin Salleh. "Extensive studies on internal and external heat transfer characteristics of integrated impingement cooling structures for HP Turbines." In *Turbo Expo: Power for Land, Sea, and Air*, vol. 43147, pp. 167-176. 2008.
<https://doi.org/10.1115/GT2008-50202>
- [2] Khalid, Amir, Shahrin Hisham Amirnordin, Latip Lambosi, Bukhari Manshoor, Mohd Farid Sies, and Hamidon Bin Salleh. "Spray characteristic of diesel-water injector for burner system." In *Advanced Materials Research*, vol. 845, pp. 66-70. Trans Tech Publications Ltd, 2014.
[10.4028/www.scientific.net/AMR.845.66](https://doi.org/10.4028/www.scientific.net/AMR.845.66)
- [3] Sapit, Azwan, Mohd Azahari Razali, Akmal Nizam Mohammed, Bukhari Manshoor, Amir Khalid, Hamidon Salleh, and Mohd Faisal Hushim. "Study on Mist Nozzle Spray Characteristics for Cooling Application." *International Journal of Integrated Engineering* 11, no. 3 (2019): 299-303.
- [4] Hashim, Muhammad Akasha, Amir Khalid, Hamidon Salleh, and Norshuhaila Mohamed Sunar. "Effects of Fuel and Nozzle Characteristics on Micro Gas Turbine System: A Review." *Proceedings of the International Research and Innovation Summit (IRIS 2017), Melaka, Malaysia* (2017): 6-7.
- [5] Amirnordin, S. H., Amir Khalid, M. F. Zailan, Mas Fawzi, Hamidon Salleh, and Izzuddin Zaman. "Thermal Imaging of Flame in Air-assisted Atomizer for Burner System." *MS&E* 226, no. 1 (2017): 012008.
[10.1088/1757-899X/226/1/012008](https://doi.org/10.1088/1757-899X/226/1/012008)
- [6] Mohd Azahari Razali, Azwan Sapit, Mohd Faizal Mohideen Batcha, Rais Hanizam Madon, Amir Khalid, Md Norrizam Mohmad Ja'at, Akmal Nizam Mohammed, Hamidon Salleh, Mohd Faisal Hushim, and Ubaidilah Ab. Hadi. "Preliminary Study of Effect of Natural Thread Distance on Angle Dependency of Flame Spread Behaviour over Kenaf/Polyester Fabric." *Journal of Advanced Research in Fluid Mechanics and Thermal Sciences* 62, no. 2 (2019): 250-255.
- [7] Padture, Nitin P., Maurice Gell, and Eric H. Jordan. "Thermal barrier coatings for gas-turbine engine applications." *Science* 296, no. 5566 (2002): 280-284.
[10.1126/science.1068609](https://doi.org/10.1126/science.1068609)
- [8] Funazaki, K., and K. Hachiya. "Systematic numerical studies on heat transfer and aerodynamic characteristics of impingement cooling devices combined with pins." In *Turbo Expo: Power for Land, Sea, and Air*, vol. 36886, pp. 185-192. 2003.
<https://doi.org/10.1115/GT2003-38256>
- [9] Cho, Hyung Hee, and Dong Ho Rhee. "Local heat/mass transfer measurement on the effusion plate in impingement/effusion cooling systems." *Journal of Turbomachinery*. 123, no. 3 (2001): 601-608.
<https://doi.org/10.1115/1.1344904>
- [10] Han, B., and Richard J. Goldstein. "Jet-impingement heat transfer in gas turbine systems." *Annals of the New York Academy of Sciences* 934, no. 1 (2001): 147-161.
[10.1615/HeatTransRes.v42.i2.30](https://doi.org/10.1615/HeatTransRes.v42.i2.30)
- [11] Garimella, Suresh V., and Boris Nenyadykh. "Nozzle-geometry effects in liquid jet impingement heat transfer." *International Journal of Heat and Mass Transfer* 39, no. 14 (1996): 2915-2923.
[https://doi.org/10.1016/0017-9310\(95\)00382-7](https://doi.org/10.1016/0017-9310(95)00382-7)
- [12] Ekkad, Srinath V., Yizhe Huang, and Je-Chin Han. "Impingement heat transfer on a target plate with film cooling holes." *Journal of Thermophysics and Heat transfer* 13, no. 4 (1999): 522-528.
<https://doi.org/10.2514/2.6471>
- [13] L.W. Florschuetz and C.C. Su. "Effects of Crossflow Temperature on Heat Transfer within an Array of Impinging Jets" *ASME Journal of Heat Transfer* 101 (1979): 526-531.
- [14] Yamawaki, Shigemichi, Chiyuki Nakamata, Ryouji Imai, Shinsuke Matsuno, Toyoaki Yoshida, Fujio Mimura, and Masaya Kumada. "Cooling performance of an integrated impingement and pin fin cooling configuration." In *Turbo Expo: Power for Land, Sea, and Air*, vol. 36886, pp. 133-142. 2003.
<https://doi.org/10.1115/GT2003-38215>
- [15] Metzger, D. E., R. A. Berry, and J. P. Bronson. "Developing heat transfer in rectangular ducts with staggered arrays of short pin fins." (1982): 700-706.
<https://doi.org/10.1115/1.3245188>
- [16] Funazaki, K., Y. Tarukawa, T. Kudo, S. Matsuno, R. Imai, and S. Yamawaki. "Heat transfer characteristics of an integrated cooling configuration for ultra-high temperature turbine blades: experimental and numerical investigations." In *Turbo Expo: Power for Land, Sea, and Air*, vol. 78521, p. V003T01A031. American Society of Mechanical Engineers, 2001.
<https://doi.org/10.1115/2001-GT-0148>
- [17] Han, Je-Chin, Sandip Dutta, and Srinath Ekkad. *Gas turbine heat transfer and cooling technology*. CRC press, 2012.

- <https://doi.org/10.1201/b13616>
- [18] Cengel, Yunus A., and Michael A. Boles. *Thermodynamics: An Engineering Approach 6th Edition (SI Units)*. The McGraw-Hill Companies, Inc., New York, 2007.
- [19] Al-Hadhrami, Luai M., S. Shaahid, and Ali A. Al-Mubarak. "Jet impingement cooling in gas turbines for improving thermal efficiency and power density." *Advances in Gas Turbine Technology* (2011): 191-210.
- [20] Dutta, T., K. P. Sinhamahapatra, and S. S. Bandyopdhyay. "Comparison of different turbulence models in predicting the temperature separation in a Ranque–Hilsch vortex tube." *international journal of refrigeration* 33, no. 4 (2010): 783-792.
[10.1016/j.ijrefrig.2009.12.014](https://doi.org/10.1016/j.ijrefrig.2009.12.014)
- [21] Bartosiewicz, Y., Zine Aidoun, P. Desevaux, and Yves Mercadier. "CFD-experiments integration in the evaluation of six turbulence models for supersonic ejectors modeling." In *Integrating CFD and Experiments Conference, Glasgow, UK*. 2003.
- [22] Bartosiewicz, Yann, Z. Aidoun, and Y. Mercadier. "Numerical assessment of ejector operation for refrigeration applications based on CFD." *Applied thermal engineering* 26, no. 5-6 (2006): 604-612.
<https://doi.org/10.1016/j.applthermaleng.2005.07.003>
- [23] Karmare, S. V., and A. N. Tikekar. "Analysis of fluid flow and heat transfer in a rib grit roughened surface solar air heater using CFD." *Solar Energy* 84, no. 3 (2010): 409-417.
[10.1016/j.solener.2009.12.011](https://doi.org/10.1016/j.solener.2009.12.011)